

# Sensor-fusion Based Prognostics for Deep-space Habitats Exhibiting Multiple Unlabeled Failure Modes

**Benjamin Peters**

University of Texas-Rio Grande Valley, Edinburg, USA

**Ayush Mohanty**

Georgia Institute of Technology, Atlanta, USA

**Xiaolei Fang**

North Carolina State University, Raleigh, USA

**Nagi Gebrael**

Georgia Institute of Technology, Atlanta, USA

**Stephen K. Robinson**

University of California Davis, Davis, USA

**Abstract**— Deep-space habitats are complex systems that must operate autonomously over extended durations without ground-based maintenance. These systems are vulnerable to multiple, often unknown, failure modes that affect different subsystems and sensors in mode-specific ways. Developing accurate remaining useful life (RUL) prognostics is challenging, especially when failure labels are unavailable and sensor relevance varies by failure mode. In this paper, we propose an unsupervised prognostics framework that

This effort is supported by NASA under grant number 80NSSC19K1052 as part of the NASA Space Technology Research Institute (STRI) Habitats Optimized for Missions of Exploration (HOME) ‘SmartHab’ Project. Any opinions, findings, conclusions, or recommendations expressed in this material are those of the authors and do not necessarily reflect the views of the National Aeronautics and Space Administration. (Corresponding author: Ayush Mohanty)

*Dr. Benjamin Peters is with the Department of Manufacturing and Industrial Engineering, University of Texas at Rio Grande Valley, Edinburg, USA (e-mail: benjamin.peters01@utrgv.edu). Ayush Mohanty is with the School of Industrial and Systems Engineering, Georgia Institute of Technology, Atlanta, USA (e-mail: ayush.mohanty@gatech.edu). Dr. Xiaolei Fang is with the Department of Industrial and Systems Engineering, North Carolina State University, USA (e-mail: author@nrim.go.jp). Dr. Nagi Gebrael is Georgia Power professor with the School of Industrial and Systems Engineering, Georgia Institute of Technology, Atlanta, USA (e-mail: nagi.gebraeel@isye.gatech.edu). Dr. Stephen Robinson is a retired astronaut with NASA, currently serving as a professor with the Department of Mechanical and Aerospace Engineering, University of California Davis, Davis, USA (e-mail: author@nrim.go.jp).*

© 20xx IEEE. Personal use of this material is permitted. Permission from IEEE must be obtained for all other uses, in any current or future media, including reprinting/republishing this material for advertising or promotional purposes, creating new collective works, for resale or redistribution to servers or lists, or reuse of any copyrighted component of this work in other works.

0018-9251 © 2026 IEEE

jointly identifies latent failure modes and selects informative sensors using only unlabeled training data. The methodology consists of two phases. In the offline phase, we model system failure times using a mixture of Gaussian regressions and apply an Expectation-Maximization algorithm to cluster degradation trajectories and select mode-specific sensors. In the online phase, we extract low-dimensional features from the selected sensors to diagnose the active failure mode and predict RUL using a weighted regression model. We demonstrate the effectiveness of our approach on a simulated dataset that reflects deep-space telemetry characteristics and on a real-world engine degradation dataset, showing improved accuracy and interpretability over existing methods.

**Index Terms**— Deep-space Habitats, Failure Diagnosis, Multiple Failure Modes, Prognostics, Remaining Useful Life, Sensor Fusion

## I. INTRODUCTION

Deep-space habitat is a complex engineering system (CES), composed of multiple interacting subsystems that must work together to support human life and mission operations over long durations. These subsystems such as the environmental control and life support system, energy and power systems, thermal control, robotic agents, and structural components etc., must function reliably in harsh and isolated environments, where failure of any component can lead to mission-critical consequences [1], [2]. The complexity of such systems arises not only from the tight integration of these subsystems but also from their heterogeneous origins. Components are often developed by different manufacturers and tested independently, making it difficult to anticipate how they will behave once integrated. Additionally, the deep-space environment introduces operating conditions such as microgravity, radiation, and thermal extremes that differ significantly from terrestrial test settings. These novel conditions can give rise to failure modes that have never been observed during isolated ground-based validation. As a result, building a comprehensive library of failure modes becomes essential for predicting degradation behaviors (i.e., prognostics) during the mission. However, due to limited diagnostic access and the lack of labeled failure data, this library must often be inferred from unlabeled system observations.

In addition to the challenge of missing labels, deep-space habitats face another difficulty that limits their prognostic capability. These systems are typically equipped with a large number of sensors that generate in situ telemetry data to continuously monitor system health. However, analyzing this data presents several issues. Not all sensors are informative for predicting remaining useful life (RUL), and many may be redundant or affected by noise. Furthermore, in systems with multiple failure modes, sensor informativeness is often mode-specific. A sensor that is strongly predictive under one failure mode may be uninformative under another (see Figure 1). This variability complicates the task of selecting a reliable subset of sensors for prognostic modeling, especially with unknown failure modes.

In this paper, we propose a data-driven prognostics framework for deep-space systems that are monitored by

many sensors and subject to multiple, unknown failure modes. Our methodology consists of two key stages: (1) an offline sensor selection step and (2) an online diagnosis and prognostics step. These stages align with two mission stages: during early deployment, the habitat operates under limited supervision to collect historical sensor data for initializing the model; after this setup phase, autonomous health monitoring and prediction begin.

**Main Contributions.** A unique aspect of our approach is that **we do not assume failure mode labels are known in the historical training data (degradation signals)**. This reflects realistic space mission constraints, where diagnosing past failures requires expert involvement and post-mission analysis. To address this, we model failure times using a mixture of Gaussian regressions, where regressors are features extracted from sensor data. We develop a novel Expectation-Maximization (EM) algorithm that simultaneously labels failure modes and selects the most informative sensors for each mode. In the online phase, we use real-time sensor data to first diagnose the dominant failure mode before predicting RUL. We apply Multivariate Functional Principal Component Analysis (MFPCA) to extract low-dimensional, yet informative features from the mode-specific sensors identified in the offline phase. We then classify the active failure mode using a nearest-neighbor approach and apply a weighted functional regression model to predict RUL. The key technical contributions of this paper can be summarized as:

- We develop a feature extraction methodology that fuses multivariate sensor data from systems exhibiting multiple failure modes into compact and informative representations.
- We propose a failure-mode-aware sensor selection approach using an Expectation-Maximization algorithm that jointly clusters unlabeled failure events and selects informative sensors for each failure mode.
- We present an integrated online framework that uses real-time data to (1) diagnose the active failure mode and (2) predict RUL using a mode-specific regression model.
- We demonstrate the effectiveness and robustness of the proposed methodology through two case studies relevant to deep-space habitats: (1) a controlled simulation designed to reflect key telemetry challenges, and (2) a real-world NASA turbofan engine degradation dataset that mimics sensor-driven subsystem degradation in long-duration missions.

The remainder of the paper is organized as follows. Section II reviews related work on RUL prediction and multi-failure mode diagnostics. Section III introduces our proposed prognostics framework. Section IV describes the offline sensor selection method. Section V details the online diagnosis and RUL prediction approach. Section VI and Section VII present two case studies—a simulated dataset and the NASA turbofan engine dataset, respec-

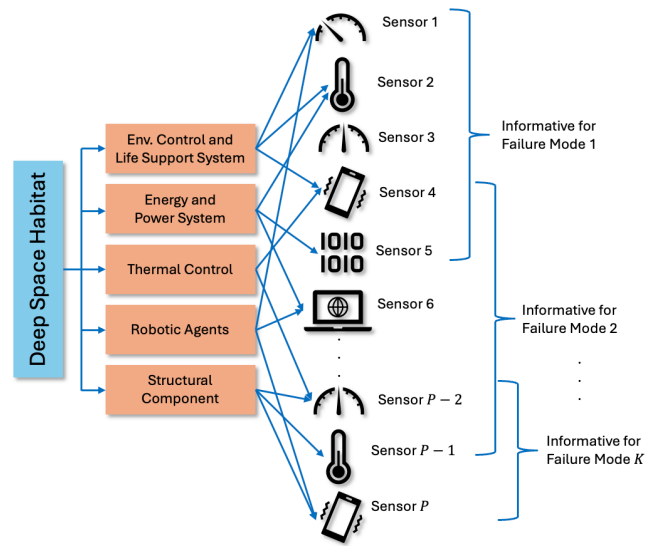


Fig. 1. Example of a deep-space habitat with multiple subsystems. Health of each subsystem is monitored by a subset of onboard sensors. The subset of informative sensors vary for different failure modes.

tively. We conclude the paper in Section VIII with a discussion of future work.

## II. LITERATURE REVIEW

Approaches for RUL prediction of CES are typically categorized as either physics-based or data-driven. Physics-based approaches [3], [4] utilize first principles to mathematically model the underlying physics of system degradation. For example, [3] used a two-stage nonlinear differential equation to model the rate of air pressure changes inside a space habitat. They use an Extended Kalman Filter (EKF) to estimate the parameters of this model and predict RUL by using the same EKF to forecast when the habitat pressure becomes untenable. In general, physics-based approaches typically develop state-space models of system degradation and use a Bayesian filter such as the Kalman Filter or the Particle Filter for real-time estimation and prediction of model parameters. Several examples of this are highlighted by [5]. The advantages of physics-based approaches include high prediction accuracy and limited need for data. However, their requirement for thorough knowledge of the physics behind system failure renders them difficult to develop, given the growing system complexity.

Conversely, data-driven approaches attempt to map sensor data to the system RUL using statistical models, machine learning, or hybrid approaches. Since sensors are monitoring the system over a prolonged period, they generate continuous, high-volume data called “streaming data.” The approaches developed for single-sensor streaming data include both statistical methods that model univariate degradation signals using exponential models [6], [7], random-coefficient regression [8], Brownian motion [9], Gamma process [10], or hidden Markov model [11] and machine learning methods that use deep learning [12],

[13] or relevance vector machine [14]. However, single-sensor approaches are not scalable to the scenario where multiple sensors monitor systems. Under this scenario, sensors produce multivariate streaming data. For this type of data, authors have developed sensor fusion algorithms that operate at either the decision level or the data level [15]. Decision-level fusion consists of systematically combining RUL estimates from different models, whereas data-level fusion synthesizes the multivariate sensor data into a univariate health indicator, which can be modeled using standard univariate techniques. Existing data fusion approaches include Principal Component Analysis [16], [17], [18], maximum likelihood methods [19], extreme learning machine [20], deep learning [21], [22], state-space models [23], [24], [25], and logistic regression [26].

While effective, many data fusion methods rely on aggregating all available sensor signals. In practice, not all sensors are informative for a given failure mechanism, and fusing irrelevant signals can introduce noise and reduce prediction accuracy. To address this, some studies incorporate sensor selection. For instance, adaptive lasso has been used to eliminate uninformative sensors [15], [19], and group regularization techniques have been applied for joint selection and modeling [18]. However, these approaches typically assume a single dominant failure mode.

In reality, most CES experience multiple failure modes, reflecting the structure and function of their sub-systems. Competing risk models have been widely used to represent such systems. Traditional approaches often rely on statistical models, such as the Cox proportional hazards model with Weibull baselines [27], [28]; a comprehensive review is provided in [29]. More recently, deep learning has also been used to model competing risks [30]. For example, both [31] and [32] both employ deep recurrent neural networks for recurrent event survival analysis with competing risks.

Competing risk models often produce survival or hazard rates that can be difficult to interpret in engineering contexts. As a result, many researchers have shifted toward methods that directly model sensor data to predict RUL, though few focus on multiple failure modes. Often, researchers develop general RUL prediction methodologies and then apply them to datasets with multiple failure modes. For example, [33] proposed a correlation and relative entropy feature engineering framework for complex systems and [34] proposed a deep convolutional neural network. In both cases, the researchers validated their methodologies on datasets with multiple failure modes. However, they do not consider multiple failure modes in an explicit manner. Failure to do so could result in highly biased predictions. Therefore, the development of RUL prediction methodologies that account for multiple failure modes is growing. [35] used a support vector machine for failure mode diagnosis with features extracted from a deep belief network, followed by RUL prediction using a particle filter. [36] trained distinct LSTM models for each failure mode. Once a

TABLE I  
Comparison of Prognostic Methodologies in the Literature

Prognostic Methodology	Sensor Fusion	Sensor Selection	Multiple Failure Modes	Unlabeled Failure Modes	Model Interpretability
[3], [4], [5]	✓	✓	✓	N/A	✓
[6], [7], [8], [9], [10], [11]	✓	✓	✓	✓	✓
[16], [17], [18], [19], [21]	✓	✓	✓	✓	Partial
[19], [18], [41]	✓	✓	✓	✓	✓
[37], [42], [35], [36]	✓	Partial	✓	✓	✓
[38]	✓	✓	✓	Partial	Partial
[39], [40]	✓	Partial	✓	✓	Partial
[30], [43], [31], [32], [44]	✓	✓	✓	✓	✓
[42], [33], [45], [34]	✓	✓	✓	✓	✓
Ours	✓	✓	✓	✓	✓

physics-informed CNN classifier diagnoses the active failure mode, the appropriate LSTM model is utilized. Furthermore, [37] fit random coefficient models to failure mode-specific health indices. However, these articles do not incorporate a sensor selection algorithm and they rely on labeling of the failure modes determined either through visual inspection or domain knowledge. Consequently, researchers have begun addressing these gaps. [38] adopted a semi-supervised graph-based approach for feature extraction from partially labeled failures and used elastic net functional regression for sensor selection and RUL prediction. More recently, [39] proposed a time-series clustering algorithm to identify latent failure modes, followed by LSTM-based RUL prediction. Furthermore, [40] combined mixture of (log)-location scale regression with deep learning to predict RUL in a scenario with unknown failure modes. However, in both papers, sensor selection was limited to excluding sensors with obviously non-informative signals, such as constant or low-variance signals.

Our methodology differs from prior work by addressing a setting in which failure mode labels are entirely unknown. We assume that each failure mode is associated with a (not necessarily disjoint) subset of sensors that are informative for RUL prediction. The goal is to develop an unsupervised prognostic framework that systematically fuses multivariate sensor signals for RUL estimation. We assume access to a historical repository of system run-to-failure trajectories, where degradation was monitored from the onset of an incipient fault to final failure using multiple sensors. Furthermore, we assume that each system fails independently and experiences only one failure mode during its lifetime. Finally, while the failure labels are unobserved, we assume that the total number of potential failure modes is known. In the following sections, we detail our prognostics framework.

### III. OVERVIEW OF THE PROGNOSTICS FRAMEWORK

This section describes our prognostics framework, developed for autonomous health monitoring in deep space habitats. A flowchart of the framework is shown in Figure 2. The framework consists of two main components: “*Offline Sensor Selection*” and “*Online Diagnosis and Prognostics*”.

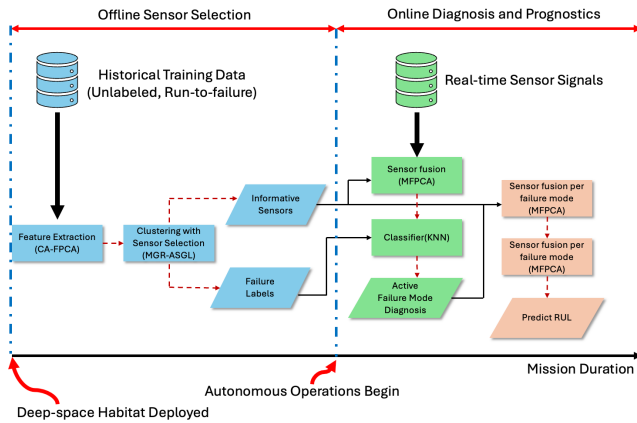


Fig. 2. Overview of the proposed prognostics framework for deep-space habitats

**I. Offline Sensor Selection:** This stage occurs shortly after the habitat is deployed, during an initial period where degradation signals are collected with limited ground or crew assistance. The data collected during this stage forms a historical dataset, which is used to initialize the prognostic models before autonomous operation begins. We assume that the dataset contains multiple failure modes, although the *failure modes are not labeled*. The goal of this step is to (1) label the degradation signals into one of the failure modes, and (2) identify a subset of informative sensors for each failure mode. This step consists of two parts discussed below:

- 1) **Feature Extraction:** The onboard sensors generate high-dimensional, time-varying signals. To extract informative features for prognostics, we use a covariate-adjusted functional principal component analysis (CA-FPCA) method. CA-FPCA models the variation in each sensor signal while accounting for external covariates. In our setting, these covariates represent the underlying failure modes, which are unknown a priori. To estimate them, we first perform a K-means clustering on the sensor signals and use the resulting cluster labels as initial covariates.
- 2) **Optimization:** After feature extraction, we obtain a reduced set of features for each sensor. These features are called CA-FPC scores. We use these scores as predictors in a mixture of Gaussian regression (MGR) model. The MGR model estimates the natural logarithm of the time-to-failure,  $\ln TTF$ , as a function of the CA-FPC scores. The model assumes that this relationship ( $\ln TTF$  vs CA-FPC scores) depends on the underlying failure mode. We fit the MGR model using the EM algorithm, which results in: (1) *optimal failure mode labels* for each sample, and (2) an *optimal subset of informative sensors* for each failure mode.

**II. Online Diagnosis and Prognostics:** Once, the failure mode labeling and sensor selection are complete,

the habitat enters into autonomous mode. This stage uses real-time sensor data to (1) identify the active failure mode and (2) predict the RUL:

- 1) **Diagnosis:** Prior to the diagnosis step, the active failure mode is unknown. Therefore, all selected sensors are utilized in this step. First we apply multivariate functional principal component analysis (MFPCA) to signals from all selected sensors to extract a compact set of features, called MFPC scores, that represent the joint behavior of all sensors. Then we classify the active failure mode by finding its K-nearest neighbors and assigning the most common failure mode among them.
- 2) **Prognostics:** Once the active failure mode is diagnosed, we recalculate the MFPC scores using only the informative sensors for that mode. A functional regression model uses these scores to predict the RUL.

#### IV. OFFLINE SENSOR SELECTION

We consider a scenario where the deep-space habitat is monitored by  $P$  different sensors. We assume there exists a historical dataset comprised of  $P$ -dimensional degradation-based sensor signals from monitoring  $N$  similar systems. We denote  $s_{i,p}(t)$  as the signal data from sensor  $p \in \{1, \dots, P\}$  for system  $i \in \{1, \dots, N\}$  observed at time  $t \in [0, T]$ , where  $T = \min(\{TTF_i\}_{i=1}^N)$ . By truncating all signals to the minimum failure time, we ensure that all signals in the training set have the same time domain and that they are all included when modeling. For this framework, we assume that the total number of failure modes,  $K$  is known, but that the actual failure labels in the training dataset are unknown. This poses a challenge for CA-FPCA, which requires observed covariates for computation. To determine these covariates, we perform a sensor-wise clustering of the training samples. For each sensor, we perform FPCA for feature extraction and then use K-means clustering with  $K$  clusters to label the signals from that sensor. Once the sensor-wise clustering is complete, the next step involves feature extraction by applying CA-FPCA and then regressing these features against the time-to-failure to identify the most informative subset of sensors for each failure mode. The next two subsections discuss details about the feature extraction (CA-FPCA), and the optimization (MGR-ASGL) model.

##### A. Feature Extraction: CA-FPCA

CA-FPCA extends conventional FPCA to handle complex data structures where the dynamics of time-varying signals are affected by one or more additional factors, i.e. covariates. In [46], the covariates are assumed to be continuous variables, and thus, mean and covariance estimation requires smoothing over both time and the covariate space. In this paper, **we use the sensor-wise cluster labels as covariates**. Let  $\mathcal{I}_p^k$  denote the set of

indices for sensor  $p$  signals assigned to cluster  $k, k \in \{1, 2, \dots, K\}$ . The CA-FPCA problem was reduced to performing FPCA on each cluster. For a given system  $i$ , signals from cluster  $k$  of sensor  $p$  are modeled as:

$$s_{i,p}(t) = v_{i,p}^k(t) + \epsilon_{i,p}(t), i \in \mathcal{I}_k^p \quad (1)$$

where  $v_{i,p}^k(t)$  is a smooth random function, and  $\epsilon_{i,p}(t)$  are assumed to be independently and identically distributed (i.i.d.) errors with mean zero and variance  $\sigma_p^2$ .  $v_{i,p}^k(t)$  and  $\epsilon_{i,p}(t)$  are assumed to be independent of each other. The mean and covariance functions of  $v_{i,p}^k(t)$  are given by  $\mu_p^k(t)$  and  $\mathbb{C}_p^k(t, t')$ , respectively. Using Mercer's theorem [47], the covariance can be decomposed as follows,  $\mathbb{C}_p^k(t, t') = \sum_{m=1}^{\infty} \lambda_{m,p}^k \phi_{m,p}^k(t) \phi_{m,p}^k(t')$ , where  $\{\phi_{m,p}^k(t)\}_{m=1}^{\infty}$  are the orthogonal eigenfunctions of  $\mathbb{C}_p^k(t, t')$  and  $\lambda_{1,p}^k \geq \dots \geq \lambda_{m,p}^k \geq \dots$  are the corresponding eigenvalues. By projecting the mean-subtracted signal data onto the eigenfunctions, we can represent the signals by Eq (2).

$$s_{i,p}(t) = \mu_p^k(t) + \sum_{m=1}^{\infty} \xi_{i,m,p}^k \phi_{m,p}^k(t) + \epsilon_{i,p}(t) \quad (2)$$

where  $\xi_{i,m,p}^k$  is the  $m$ th CA-FPC-score with mean 0 and variance  $\lambda_{m,p}^k$ . The CA-FPC scores are computed using the PACE algorithm in [48]. Since the eigenvalues decrease as  $m \rightarrow \infty$ , we can obtain a low-dimensional representation of  $s_{i,p}^k(t)$  using the first  $q_p$  CA-FPC-scores.

To ensure all features are scaled equally, we standardize the CA-FPC-scores by subtracting the sample mean and dividing by the sample standard deviation. Let  $x_{i,m}^p$  denote the standardized  $m$ th CA-FPC-score from sensor  $p$  of system  $i$ . We extract  $\mathbf{x}_{i,p} = (x_{i,1}^p, \dots, x_{i,q_p}^p)^T$  for sensor  $p$  of system  $i$ . We then utilize the  $\mathbf{x}_{i,p}$ 's as predictors for fitting the MGR-ASGL model.

## B. Optimization of the MGR-ASGL model

Let  $Y_i = \frac{\ln TTF_i - (1/N) \sum_{i=1}^N \ln TTF_i}{(1/(N-1)) \sum_{i=1}^N (\ln TTF_i - (1/N) \sum_{i=1}^N \ln TTF_i)^2}$ , for  $i = 1, 2, \dots, N$  denote the random variable corresponding to the standardized natural logarithm of the time-to-failure (i.e.,  $\ln TTF$ ) of system  $i$ . Furthermore, let  $\mathbf{Z}_i$  denote a categorical random vector of size  $K$  used to encode the unknown failure mode of system  $i$ . If failure mode  $k$  is responsible for the failure of system  $i$ , which occurs with probability  $\pi_k$ , then  $\mathbf{Z}_i[k] = 1$  and the remaining elements are zero. In our model, we posit that the relationship between  $Y_i$  and the observed features  $\mathbf{x}_i$  depends on which failure mode caused the failure of system  $i$ . Thus, we assume that the conditional distribution of  $Y_i$  given  $\mathbf{Z}_i[k] = 1$  is Gaussian with PDF:

$$f_{Y_i|\mathbf{Z}_i}(y_i|\mathbf{Z}_i[k] = 1) = \frac{1}{\sqrt{2\pi}\sigma_k} \exp\left(-\frac{1}{2\sigma_k^2}(y_i - \beta_{0,k} - \sum_{p=1}^P \mathbf{x}_{i,p}^T \boldsymbol{\beta}_{p,k})^2\right) \quad (3)$$

To find the marginal distribution of  $Y_i$  we use the law of total probability, summing over the joint distribution of

$Y_i$  and  $\mathbf{Z}_i$  as follows:

$$f_{Y_i}(y_i) = \sum_{k=1}^K \pi_k \frac{1}{\sqrt{2\pi}\sigma_k} \exp\left(-\frac{1}{2\sigma_k^2}(y_i - \beta_{0,k} - \sum_{p=1}^P \mathbf{x}_{i,p}^T \boldsymbol{\beta}_{p,k})^2\right) \quad (4)$$

Therefore, the marginal distribution of  $Y_i$  is a mixture of Gaussian regressions. The parameters of this model are  $\Theta = \{\pi_k, \beta_{0,k}, \boldsymbol{\beta}_{1,k}, \dots, \boldsymbol{\beta}_{P,k}, \sigma_k\}_{k=1}^K$ . To estimate these parameters, we seek to minimize the negative incomplete-data log-likelihood (IDLL). To ensure both scale-invariance of parameter estimation and convexity of the optimization problem in the M-step of our EM algorithm, we let  $\varphi_{0,k} = \sigma_k^{-1} \beta_{0,k}$ ,  $\boldsymbol{\varphi}_{p,k} = \sigma_k^{-1} \boldsymbol{\beta}_{p,k}$ , and  $\rho_k = \sigma_k^{-1}$  (see: [41]). Thus, the parameters are now  $\Theta = \{\boldsymbol{\pi}, \boldsymbol{\rho}, \boldsymbol{\varphi}\}$ , where  $\boldsymbol{\pi} = \{\pi_k\}_{k=1}^K$ ,  $\boldsymbol{\rho} = \{\rho_k\}_{k=1}^K$ , and  $\boldsymbol{\varphi} = \{\boldsymbol{\varphi}_{0,k}, \boldsymbol{\varphi}_{1,k}, \dots, \boldsymbol{\varphi}_{P,k}\}_{k=1}^K$ . Assuming that  $Y_1, \dots, Y_N$  are independent, the negative IDLL is computed as follows:

$$-\ell(\Theta|\mathbf{Y}) = -\sum_{i=1}^N \ln \left[ \sum_{k=1}^K \pi_k \rho_k \frac{1}{\sqrt{2\pi}} \exp\left(-\frac{1}{2}(y_i \rho_k - \varphi_{0,k} - \sum_{p=1}^P \mathbf{x}_{i,p}^T \boldsymbol{\varphi}_{p,k})^2\right) \right] \quad (5)$$

Estimating  $\Theta$  requires minimizing Eq 5. However, the logarithm inside the summation makes Eq 5 difficult to optimize globally. Instead, we search for a local minimum using the EM algorithm, an iterative algorithm suitable for fitting probability models with latent variables. To utilize the EM algorithm, we first construct the negative complete-data log likelihood (CDLL).

$$\begin{aligned} -\ell_C(\Theta|\mathbf{Y}, \mathbf{Z}) &= -\ln \left( \prod_{i=1}^N \prod_{k=1}^K f_{Y_i}(y_i)^{\mathbf{Z}_i[k]} \right) \\ &= -\sum_{i=1}^N \sum_{k=1}^K \mathbf{Z}_i[k] \ln \left[ \pi_k \rho_k \frac{1}{\sqrt{2\pi}} \exp\left(-\frac{1}{2}(y_i \rho_k - \varphi_{0,k} - \sum_{p=1}^P \mathbf{x}_{i,p}^T \boldsymbol{\varphi}_{p,k})^2\right) \right] \end{aligned} \quad (6)$$

In Appendix A, we show that the expectation of the negative CDLL with respect to the conditional distribution of  $\mathbf{Z}$  given  $\mathbf{Y}$  forms an upper bound for the negative IDLL. Therefore, we can obtain a local minimum by minimizing this upper bound. The proposed EM algorithm is performed as follows:

1) **Initialization:** Set the initial parameters to  $\Theta^{(0)}$  s.t.,

$$\Theta^{(0)} = \{\pi_k^{(0)}, \varphi_{0,k}^{(0)}, \boldsymbol{\varphi}_{1,k}^{(0)}, \dots, \boldsymbol{\varphi}_{P,k}^{(0)}, \rho_k^{(0)}\}_{k=1}^K \quad (7)$$

- 2) **E-step:** Given  $\Theta^{(m)}$ , the expectation of  $-\ell_C(\Theta|\mathbf{Y}, \mathbb{Z})$  is given as:

$$\begin{aligned} Q(\Theta, \Theta^{(m)}) &= \mathbb{E}[-\ell_C(\Theta|\mathbf{Y}, \mathbb{Z})|\mathbf{Y}, \Theta^{(m)}] \\ &= -\sum_{i=1}^N \sum_{k=1}^K \gamma_{i,k} \ln \left[ \pi_k \rho_k \frac{1}{\sqrt{2\pi}} \exp \left( -\frac{1}{2} (y_i \rho_k - \varphi_{0,k} - \sum_{p=1}^P \mathbf{x}_{i,p}^T \varphi_{p,k})^2 \right) \right] \end{aligned} \quad (8)$$

where,

$$\begin{aligned} \gamma_{i,k} &:= \mathbb{E}(\mathbf{Z}_i[k] | Y_i = y_i, \Theta^{(m)}) \\ &= \Pr(\mathbf{Z}_i[k] = 1 | Y_i = y_i, \Theta^{(m)}) \\ &= \frac{\pi_k^{(m)} \rho_k^{(m)} \frac{1}{\sqrt{2\pi}} \exp \left( -\frac{1}{2} (y_i \rho_k^{(m)} - \varphi_{0,k}^{(m)} - \sum_{p=1}^P \mathbf{x}_{i,p}^T \varphi_{p,k}^{(m)})^2 \right)}{\sum_{l=1}^K \pi_l^{(m)} \rho_l^{(m)} \frac{1}{\sqrt{2\pi}} \exp \left( -\frac{1}{2} (y_i \rho_l^{(m)} - \varphi_{0,l}^{(m)} - \sum_{p=1}^P \mathbf{x}_{i,p}^T \varphi_{p,l}^{(m)})^2 \right)} \end{aligned} \quad (9)$$

is the responsibility that failure mode  $k$  takes for the failure of system  $i$ . These responsibilities enable a soft clustering, where we claim system  $i$  failed due to failure mode  $k$  if  $\gamma_{i,k} > \gamma_{i,l}$  for  $l \neq k$ .

- 3) **M-Step:** After computing the responsibilities  $\gamma_{i,k}$ , we can update our estimate of  $\Theta$  by maximizing  $Q(\Theta, \Theta^{(m)})$  with respect to  $\Theta$ . To perform sensor selection, we augment  $Q(\Theta, \Theta^{(m)})$  with the adaptive sparse group lasso penalty and form the following optimization problem:

$$\begin{aligned} \min_{\Theta} \left\{ Q(\Theta, \Theta^{(m)}) + \lambda \sum_{k=1}^K \pi_k \left( \alpha \sum_{p=1}^P \|\varphi_{p,k}\|_1 \right. \right. \\ \left. \left. + (1 - \alpha) \sum_{p=1}^P \sqrt{q_p} \|\varphi_{p,k}\|_2 \right) \right\} \end{aligned} \quad (10)$$

We refer to the problem in Eq 10 as Mixture of Gaussian Regression–Adaptive Sparse Group Lasso (MGR-ASGL). Because  $\pi$  is included in the penalty, we follow [49] and use a two-step optimization:

- **Step 1: Improvement w.r.t.  $\pi$**

We start by using the responsibilities from the E-step to identify a feasible solution  $\bar{\pi}^{(m+1)} = \left( \frac{1}{N} \sum_{i=1}^N \gamma_{i,1}, \dots, \frac{1}{N} \sum_{i=1}^N \gamma_{i,K} \right)^T$ . Then, we update the mixing coefficients as follows:

$$\boldsymbol{\pi}^{(m+1)} = \boldsymbol{\pi}^{(m)} + u_m (\bar{\boldsymbol{\pi}}^{(m+1)} - \boldsymbol{\pi}^{(m)}) \quad (11)$$

where  $u_m \in (0, 1]$  is chosen to be the largest value in the sequence  $\{1, \frac{1}{2}, \frac{1}{4}, \dots\}$  such that the objective function does not increase.

- **Step 2: Improvement w.r.t.  $\rho$  and  $\varphi$**

Given the updated mixing coefficients, we can optimize Eq 10 with respect to the other parameters. It can be shown that this problem can be decomposed into solving  $K$  individual problems, one for each failure mode. Therefore, for  $k = 1, \dots, K$ , we solve

$$\begin{aligned} \min \left\{ -\sum_{i=1}^N \gamma_{i,k} \left[ \ln \pi_k^{(m+1)} + \ln \rho_k \right. \right. \\ \left. \left. - \frac{1}{2} (y_i \rho_k - \varphi_{0,k} - \sum_{p=1}^P \mathbf{x}_{i,p}^T \varphi_{p,k})^2 \right] \right. \\ \left. + \lambda \pi_k^{(m+1)} \left( \alpha \sum_{p=1}^P \|\varphi_{p,k}\|_1 \right. \right. \\ \left. \left. + (1 - \alpha) \sum_{p=1}^P \sqrt{q_p} \|\varphi_{p,k}\|_2 \right) \right\} \end{aligned} \quad (12)$$

Note that the tuning parameters  $\lambda$  and  $\alpha$  do not change for different  $k$ . These parameters can be selected using cross-validation. When  $\lambda$  increases, ASGL drives groups of regression coefficients to zero. Since these groups correspond to features extracted from individual sensors, this, in effect, causes the influence of some sensors to vanish. Therefore, a sensor is considered significant for failure mode  $k$  if  $\|\varphi_{p,k}\|_2 \neq 0$ . The parameter  $\alpha$  allows for some of the coefficients in a group to drop to zero to improve prediction accuracy. Finally, incorporating the adaptive parameters  $q_p$  and  $\gamma_{i,k}$  into the penalty ensures that sensor selection is not affected by class imbalance and the dimensionality of the features. Let  $\boldsymbol{\rho}^{(m+1)}$  and  $\boldsymbol{\varphi}^{(m+1)}$  denote the solution to Eq 12. Thus, after completing Steps 1 and 2, we have our updated solution  $\Theta^{(m+1)} = \{\boldsymbol{\pi}^{(m+1)}, \boldsymbol{\rho}^{(m+1)}, \boldsymbol{\varphi}^{(m+1)}\}$ .

Set  $\Theta^{(m+1)} \leftarrow \Theta$  and return to (1). Perform successive iterations of (1)–(3) until convergence.

## V. ONLINE DIAGNOSIS AND PROGNOSTICS

In this section, a system within a deep-space habitat is considered to be degrading in real-time. Our goal is to predict the RUL of the system. We begin by showing how to fuse the signals from multiple sensors into a parsimonious set of features. Then, we demonstrate how we utilize the fused sensor information to i) diagnose the active failure mode of the degrading system in real-time, and ii) predict its RUL.

## A. Sensor Fusion: MFPCA

Without loss of generality, let us redefine the sensor index as  $\{1, 2, \dots, \mathcal{P}\}$ , where  $\mathcal{P}$  is number of sensors we seek to fuse. Now assume that we have monitored the degrading system for a duration given by the time interval  $[0, t^*]$ . Since we are interested in RUL, we only use signals from training systems with failure times greater than  $t^*$ . We define this set as the “ $t^*$ -training” set, whose indices we denote by the set  $\mathcal{I}_{t^*}$ , which has cardinality  $N_{t^*}$ . Furthermore, we smooth the degradation signals using the ‘rloess’ method as described in [50]. This method uses weighted least squares with a 2nd-order polynomial for smoothing. The weights come from a bisquare weight function requiring a specified bandwidth parameter. This method also identifies outliers and assigns them weights of zero to improve signal mean estimation. To perform MFPCA, we model the  $i$ th smoothed multivariate signal evaluated at time  $t \in [0, t^*]$  as having mean  $\boldsymbol{\mu}(t) \in \mathcal{R}^{\mathcal{P}}$  and  $\mathcal{P} \times \mathcal{P}$  block covariance function  $\mathcal{C}(t, t')$ , where  $\mathcal{C}_{j, j'}(t, t') = \text{cov}(v_j(t), v_{j'}(t'))$ . Using Mercer’s theorem [47], we can represent the covariance function as  $\mathcal{C}(t, t') = \sum_{h=1}^{\infty} \eta_h \boldsymbol{\varpi}_h(t) \boldsymbol{\varpi}_h(t')^T$ , where  $(\eta_h, \boldsymbol{\varpi}_h(t))$  are the  $h$ th eigenvalue-eigenfunction pair and  $\eta_1 \geq \eta_2 \geq \dots$ . Using the first  $H$  multivariate eigenfunctions, we can represent the multivariate signal by Eq 13 where the MFPC-scores  $\zeta$ ’s are computed according to Eq 14.

$$\mathbf{s}_i(t) = \boldsymbol{\mu}(t) + \sum_{h=1}^H \zeta_{i,h} \boldsymbol{\varpi}_h(t) + \boldsymbol{\epsilon}_i(t), \quad (13)$$

$$\zeta_{i,h} = \int_0^{t^*} (\mathbf{s}_i(t) - \boldsymbol{\mu}(t))^T \boldsymbol{\varpi}_h(t) dt \quad (14)$$

In practice, we perform MFPCA by collecting the  $N_{t^*}$  observations, each consisting of the  $\mathcal{P}$  sensor signals concatenated into a single vector. Then we perform traditional PCA on the sample of observations. Furthermore, we standardize the extracted MFPC-scores so they have zero mean and unit variance.

## B. Failure Mode Diagnosis: K-nearest Neighbors

In order to diagnose the failure mode of a degrading system at time  $t^*$ , we apply MFPCA on the  $t^*$  training dataset. Next, K nearest neighbors (KNN) is applied to the standardized MFPC-scores to identify the active failure mode. Here, the distance metric of the KNN classifier is defined using the Euclidean distance between the MFPC-scores. Given this diagnosis, we now develop a model for predicting system RUL.

## C. RUL Prediction: Weighted Functional Regression

To predict RUL, we use a weighted time-varying functional regression model that maps multivariate signal features to the  $\ln TTF$ . First, we discuss the basics of a time-varying functional regression and then motivate the case for a weighted version of the model

### 1. Time-Varying Functional Regression

When predicting RUL, we are often faced with updating the relationship between time-to-failure and the current values of the extracted signal features (MFPC-scores). The predictor trajectories up to the current time are represented by time-varying MFPC-scores, which are continuously updated as time progresses and are considered to be time-varying predictor variables for the functional regression model. This is referred to as *time-varying functional regression*. It was first proposed by [51] and has been used for prognostics in [52], [18]. In our problem setting, let  $k^*$  denote the diagnosed failure mode and  $\mathcal{I}_{t^*}^{k^*} \subset \mathcal{I}_{t^*}$  denote the set of indices for training systems that failed due to failure mode  $k^*$ , but survived up to time  $t^*$ . Furthermore, let  $\mathcal{P}_{k^*} \subset \{1, 2, \dots, \mathcal{P}\}$  denote the set of sensors selected (identified as most informative) for failure mode  $k^*$ . To predict RUL, we fit a functional regression model as shown in Eq (15), where  $y_i = \ln TTF_i$ ,  $\varphi_0^{k^*}$  is the bias term,  $\boldsymbol{\varphi}^{k^*}(t) \in \mathcal{R}^{|\mathcal{P}_{k^*}|}$  is the multivariate coefficient function, and  $\mathbf{s}_i^{k^*}(t)$  is the multivariate signal consisting only of sensors significant to failure mode  $k^*$ .

$$\min_{\varphi_0^{k^*}, \boldsymbol{\varphi}^{k^*}(t)} \sum_{i \in \mathcal{I}_{t^*}^{k^*}} \left( y_i - \varphi_0 - \int_0^{t^*} \boldsymbol{\varphi}^{k^*}(t)^T \mathbf{s}_i^{k^*}(t) dt \right)^2 \quad (15)$$

We expand the coefficient function using the eigenfunctions obtained from applying MFPCA on the training set  $\mathcal{I}_{t^*}^{k^*}$ . The regression coefficient function can now be expanded as shown in Eq (16), where  $H_{k^*}$  denotes the number of MFPC-scores that were retained for failure mode  $k^*$ .

$$\boldsymbol{\varphi}(t) = \sum_{h=1}^{H_{k^*}} c_h^{k^*} \boldsymbol{\varpi}_h^{k^*}(t) \quad (16)$$

Likewise, we expand the multivariate signals using the eigenfunctions as shown in Eq (17).

$$\mathbf{s}_i^{k^*}(t) = \boldsymbol{\mu}^{k^*}(t) + \sum_{h=1}^{H_{k^*}} \zeta_{i,h}^{k^*} \boldsymbol{\varpi}_h^{k^*}(t) \quad (17)$$

Since the eigenfunctions are orthogonal, substituting Eqs (16) and (17) into Eq (15) yields the following optimization problem,

$$\min_{c_0^{k^*}, c_1^{k^*}, \dots, c_{H_{k^*}}^{k^*}} \sum_{i \in \mathcal{I}_{t^*}^{k^*}} \left( y_i - c_0^{k^*} - \sum_{h=1}^{H_{k^*}} \zeta_{i,h}^{k^*} c_h^{k^*} \right)^2 \quad (18)$$

where,

$$c_0^{k^*} = \varphi_0^{k^*} + \int_0^{t^*} \sum_{h=1}^{H_{k^*}} c_h^{k^*} \boldsymbol{\varpi}_h^{k^*}(t)^T \boldsymbol{\mu}^{k^*}(t) dt \quad (19)$$

**Weighted Version:** The offline sensor selection algorithm is unlikely to cluster failures perfectly. Therefore, when fitting the regression model, it is possible that sample systems that failed due to other failure modes are included. These systems may present themselves as outliers, compromising RUL prediction accuracy. To address this issue, we use weighted least squares to fit the time-varying functional regression model. To derive the weights, we first measure the Euclidean distance between the MFPC score of each training system to the centroid

of the cluster of the diagnosed failure mode. Then we calculate the reciprocal of that distance to define the corresponding weights for each system in the training set. If a training system's failure mode is misclassified, its corresponding weight  $w_i$  would be large, and thus, training system  $i$  would be assigned a smaller weight in the regression problem. Next, we regress the standardized  $\ln TTF$  on the MFPC-scores using a penalized weighted linear regression shown in Eq (20). For variable selection, we include the lasso penalty in the optimization problem. To ensure a regression coefficient represents the significance of their respective predictor to the prediction of the failure time, Eq (20) should be read such that  $\zeta_{i,h}^{k^*}$  is standardized.

$$\min_{c_0^{k^*}, c_1^{k^*}, \dots, c_{H_{k^*}}^{k^*}} \sum_{i \in \mathcal{I}_{i^*}^{k^*}} \left( \sqrt{w_i} y_i - \sqrt{w_i} c_0^{k^*} - \sum_{h=1}^{H_{k^*}} \sqrt{w_i} \zeta_{i,h}^{k^*} c_h^{k^*} \right)^2 + \lambda \sum_{h=1}^{H_{k^*}} \|c_h^{k^*}\| \quad (20)$$

## 2. RUL prediction

As we have shown, MFPCA enables the transformation of the functional regression problem into a multiple linear regression problem, which allows us to solve the problem by estimating only  $H_{k^*} + 1$  parameters. After fitting the regression coefficients, we extract the MFPC-scores for the test signal  $\zeta_{test,1}^{k^*}, \dots, \zeta_{test,H_{k^*}}^{k^*}$ . These MFPC scores are standardized using the sample mean and sample standard deviation of the MFPC scores from the training set. These scores are then used to predict the RUL at time  $t^*$  using Eq (21).

$$RUL_{test} = \exp \left( \left[ c_0^{k^*} + \sum_{k=1}^{H_{k^*}} \zeta_{test,h}^{k^*} c_k^{k^*} \right] \times \left[ (1/(N-1)) \sum_{i=1}^N (\ln TTF_i - (1/N) \sum_{i=1}^N \ln TTF_i)^2 \right] + (1/N) \sum_{i=1}^N \ln TTF_i \right) - t^* \quad (21)$$

## VI. CASE STUDY 1: SIMULATED DATASET

We present a simulation study that mimics the operational and diagnostic challenges of a deep-space habitat. In such systems, critical subsystems like life support, power generation, etc., are monitored by numerous sensors, and degradation can occur through multiple unknown failure modes. Due to the scarcity of in-mission failure data and the infeasibility of performing full-scale failure testing in space, simulation-based validation is pursued in this case study. This study enables us to systematically evaluate our methodology's ability to: (1) identify latent failure modes in unlabeled multivariate

sensor data, (2) select informative sensors specific to each mode, and (3) accurately predict RUL.

To emulate the complex telemetry environment of deep-space habitats, we use a modified version of the simulation model from [18] to generate degradation signals for engineered systems monitored by 20 sensors. Each system is assumed to experience one of two possible failure modes, FM 1 or FM 2, with only a subset of sensors being informative for degradation under each mode. This setup reflects the sensor redundancy and noise similar to onboard telemetry in a deep space habitat. We generate data for 200 systems per failure mode, using 160 systems for training and 40 for testing. To evaluate the robustness of our methodology, we simulate varying signal-to-noise ratios (SNRs) to mimic differences in sensor quality and environmental interference expected in long-duration missions. The resulting dataset includes multivariate sensor signals and the true time-to-failure (TTF), used for assessing prediction accuracy.

## A. Simulation Model

The signals of the underlying degradation process for system  $i$  exhibiting failure mode  $k$  are generated according to Eq (22). The signal is parameterized by the random coefficient  $\theta_i^k \sim N(\mu_k, 0.1^2)$ , which is used to control the degradation rate. We let  $\mu_1 = 1$ , and  $\mu_2 = 0.8$  be the degradation rates for FM 1 and FM 2, respectively. The TTF is computed as the first time the degradation signal  $s_i^k(t)$  crosses a soft failure threshold  $D_k$ . We set the failure thresholds for FM 1 and FM 2 as  $D_1 = 2$  and  $D_2 = 1.5$ , respectively.

$$s_i^k(t) = -\frac{\theta_i^k}{\ln t} \quad (22)$$

We consider a scenario where only a subset of sensors is correlated with the underlying degradation process associated with a given failure mode. These sensors are the informative sensors and their signal trends reflect the severity and progression of the degradation process. Note that sensors that do not exhibit any consistent trends leading up to a failure event are deemed noninformative. We define  $\mathcal{J}_k$  as the index set of informative sensors for failure mode  $k$ , and  $\mathcal{N}_k$  as the set of noninformative sensors such that  $\mathcal{N}_k \cap \mathcal{J}_k = \{\}$  (null set). Out of the 20 sensors, we set  $\mathcal{J}_1 = \{5, 12, 16, 19\}$  as the set of informative sensors for FM 1 and  $\mathcal{J}_2 = \{3, 7, 9, 19\}$  as the set of informative sensors for FM 2. The  $p^{th}$  sensor signal for the  $i^{th}$  system exhibiting failure mode  $k$  is generated using Eq (23).

$$s_{i,p}^k(t) = -\frac{\theta_{i,p}^k}{\ln t} + \epsilon_{i,p}^k(t) \quad (23)$$

In this equation,  $\epsilon_{i,p}^k(t) \sim N(0, (\sigma_p^k)^2)$  is a white noise process parameterized by  $\sigma_p^k = \mu_k / SNR_p^k$ , where  $SNR_p^k$  is the SNR for sensor  $p$  and failure mode  $k$ . To account for the correlation between the signal trends of the informative sensors and the underlying degradation

process, we generate  $\theta_{i,p}^k$  from the following conditional distribution  $\theta_{i,p}^k \mid \theta_i^k \sim N\left(\mu_k \left(1 - \sqrt{1 - \rho_p^k}\right), (0.1)^2\right)$  such that the correlation,  $\rho_p^k$ , is uniformly sampled from the interval  $[0.80, 0.99]$ . The process for generating signals for the noninformative sensors is similar to that of the informative sensors, except the interval from which we sample  $\rho_p^k$  is  $[0.1, 0.6]$ . Finally, we randomly assign a sign to  $\theta_{i,p}^k$  to allow for signals that increase or decrease in response to degradation.

In this simulation, we seek to test the robustness of our methodology to various levels of signal noise. Therefore, we generate three datasets, each with a unique interval from which to sample  $SNR_p^k$ . For  $p \in \mathcal{J}_k$ ,  $SNR_p^k$  is sampled uniformly from  $[2, 5]$ ,  $[5, 8]$ , and  $[8, 11]$  for datasets 1, 2, and 3, respectively. For  $p \in \mathcal{N}_k$ ,  $SNR_p^k$  is sampled uniformly from  $[1, 3]$  for all three datasets. Figure 3 displays samples of our sensor signals in a  $3 \times 4$  grid. Each row displays signals from four sensors (1, 3, 5, 19) for a particular SNR. Sensor 1 is not informative for either failure mode so no discernible trend is present. Sensors 3 and 5 are informative for FM 2 and FM 1, respectively. For these sensors, one signal trends downward due to degradation while the other signal appears to resemble random noise. Finally, for sensor 19, the signal decreases in response to both failure modes.

## B. Failure Mode Labeling and Sensor Selection

We analyze the ability of the MGR-ASGL model to accurately cluster the degradation signals into one of the two possible failure modes along with selecting the subset of informative sensors. We start by utilizing CA-FPCA as mentioned in A to extract features for each sensor separately. To determine the number of CA-FPC scores to retain, we use the 95% fraction of variance explained (FVE) criterion. For each cluster, we select the first  $q_p^k$  CA-FPC-scores whose eigenvalues sum to at least 0.95. Since the number of CA FPC scores to retain can vary for each cluster, we retain the maximum of  $q_p^k$  over both failure modes. For the remainder of this paper, we use 95% FVE criterion for determining the number of FPC scores, CA-FPC scores, and MFPC scores to retain. The CA-FPC scores serve as inputs to the MGR-ASGL model. Since this model has two tuning parameters, we utilize 5-fold cross-validation with  $\lambda \in \{0.0050, 0.0258, 0.0466, \dots, 0.3792, 0.4000\}$  and  $\alpha \in \{0.00, 0.25, 0.50, 0.75, 1.00\}$ . We use minimum mean-squared error (minMSE) criterion, which selects the tuning parameters that minimize the mean-squared prediction error averaged over all folds. Table II displays the tuning parameter selection using both criteria over all three datasets. For each dataset and criterion, we fit the MGR-ASGL model using these tuning parameters. We then evaluate the performance of the MGR-ASGL model on the three datasets. While clustering is an unsupervised learning task, we know the ground truth regarding the failure modes. Therefore, we evaluate the ability of the

clustering algorithm to match the ground truth. Furthermore, we have predetermined which sensors are most informative and we would like to determine whether or not the MGR-ASGL selects these sensors. The results of this performance evaluation are shown in Table III.

For all scenarios, the initial failure mode labels were determined randomly. Table II shows that for the lowest and the highest SNRs, the clustering algorithm was capable of achieving at worst 78.8% accuracy for a particular failure mode. The exception is the dataset [5,8], where the algorithm has low accuracy at clustering. This is due to the tuning parameter combination resulting in minimal coefficient shrinkage that enabled the nonsignificant sensors to influence cluster assignments. A slightly larger  $\lambda$  value would decrease this error. For all three models, several sensors that are deemed "noninformative" were selected. This can be attributed to some of these sensors having high values of  $\rho_p^k$  relative to the specified range of  $[0.1, 0.6]$ . However, simply reporting the sensors selected does not account for how informative they are. Table IV reports the four sensors with the highest  $l_2$ -norm of the regression coefficients associated with that sensor. Except for the [5,8] dataset, at least three of the four sensors with the largest  $l_2$ -norm for each failure mode are elements of the set of informative sensors. This indicates that the MGR-ASGL model results in the informative sensors having larger regression coefficients (in magnitude) than the noninformative sensors. Given the selected sensors, we want to test the robustness of the online portion of the methodology to predict remaining life.

## C. RUL Prediction

Each of the datasets consist of 80 test systems (40 from each failure mode). For each test system, we observe degradation up until the following life percentiles (in retrospect): 10%, 20%, 30%, 40%, 50%, 60%, 70%, 80%, and 90%. We smooth the training and the test signals using a bandwidth parameter of 0.5. Next, we perform MFPCA selecting the number using only the training systems that survived up to the observation time  $t^*$  corresponding to each life percentile. For a given test signal, we calculate its MFPC scores. The active failure mode is diagnosed by being assigned to the most frequent failure mode present in its closest  $0.1N_{t^*}$  neighbors. Once the active failure mode is identified, the MFPC scores of the test signals are updated and recomputed using the subset of training signals associated with the active failure mode. Next, we fit the weighted regression model and predict the RUL using the scores of the test signal. Prediction accurately is calculated retrospectively. We compute the "Estimated Life" as the current operating time plus the predicted RUL. A relative error is then computed using Eq (24).

$$\text{Relative Error} = \frac{|\text{Estimated Life} - \text{Actual Life}|}{\text{Actual Life}} \times 100\% \quad (24)$$

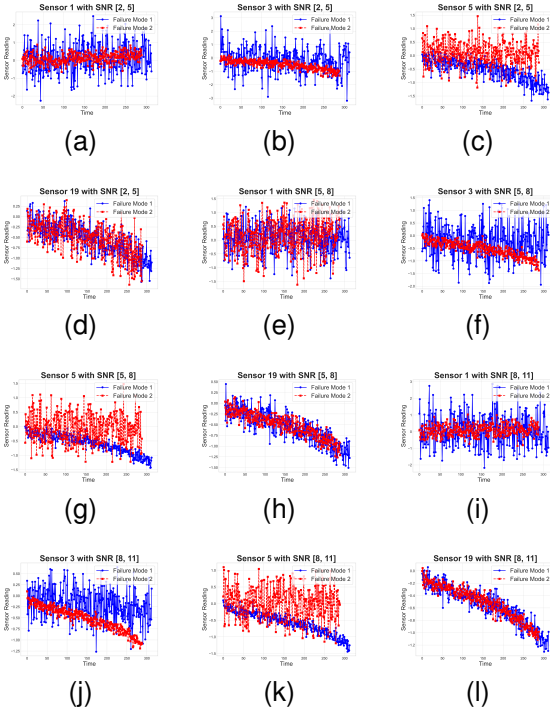


Fig. 3. Case study 1 data: Signals in sensors 1, 3, 5, 19 (columns 1, 2, 3, 4 respectively) for FM 1 and 2 under different SNRs – [2, 5], [5, 8], and [8, 11] (rows 1, 2, 3 respectively)

The performance of our methodology on predicting RUL is shown in Figure 4. In this figure, the relative errors have a generally decreasing trend for all datasets, with the [8,11] dataset tending to have smaller relative errors on average. Furthermore, the variability appears to be much larger when making predictions early in the system’s life rather than later. Interestingly, the relative error increased for the [8,11] dataset when making predictions at 90% of the system’s life. This increase may be attributed to the increased influence of incorrectly clustered training samples affecting the RUL prediction. Since this dataset has less noise, the influence of clustering may be more pronounced compared to the noisier datasets, especially if training samples have been removed for failing before 90% of the monitored system’s lifetime.

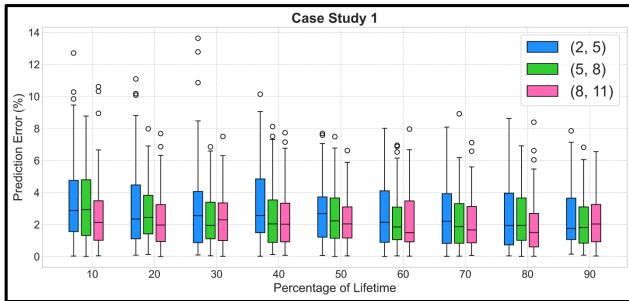


Fig. 4. Prediction error (in %) for all test systems of case study 1 under three different SNRs i.e., [2, 5], [5, 8], and [8, 11]

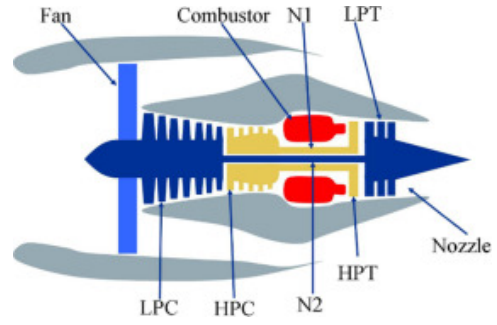


Fig. 5. The system diagram used in Case Study 2 adapted from [53]

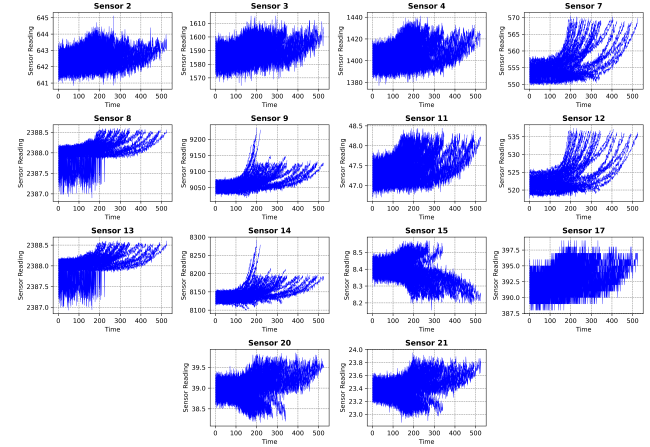


Fig. 6. Raw sensor data used for offline step in case study 2. The data is inherently unlabeled i.e., failure modes are not known.

## VII. CASE STUDY 2: NASA TURBOFAN ENGINE DATASET

To further validate our methodology in a realistic operational context, we evaluate its performance on a benchmark dataset that closely mirrors subsystem degradation in deep-space habitats. Specifically, we apply our approach to NASA’s Commercial Modular Aero-Propulsion System Simulation (C-MAPSS) dataset [53]. C-MAPSS simulates degradation in the components of turbofan engines that share telemetry and fault characteristics with propulsion and environmental control systems

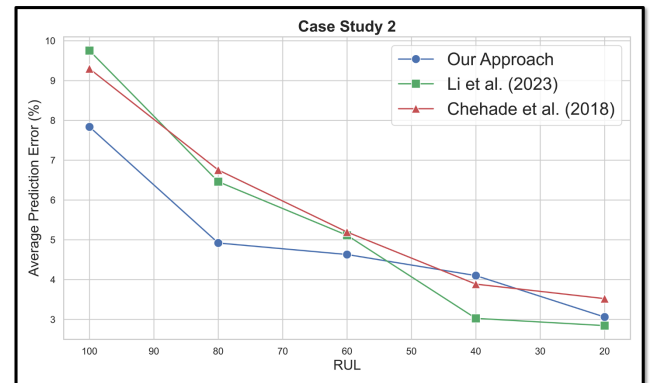


Fig. 7. Average Prediction error (%) in case study 2 with comparison to [38], and [37]

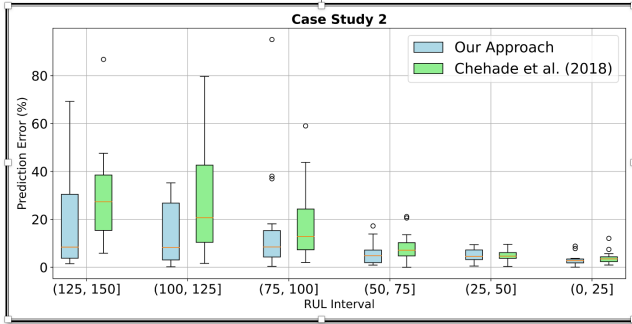


Fig. 8. Prediction error (%) for different RUL intervals in case study 2 with comparison to [37]

TABLE II  
Tuning parameter selection for case study 1

$SNR_p^k$	[2,5]	[5,8]	[8,11]
$\lambda$	0.0466	0.0258	0.0258
$\alpha$	1	0	0.25

of deep space habitats. C-MAPSS involves multivariate sensor monitoring from healthy operation to system failure, with no explicit failure mode labels and only partial degradation histories for test systems. Figure 5 displays a diagram of this turbofan engine.

In this paper, we utilize *C-MAPSS-3*, which consists of both a training and a test set. Both sets contain 100 observed engine failures caused by either fan degradation or high-pressure compressor degradation. Furthermore, both sets contain data from 21 sensors, which are listed in Table V. The signals for these sensors are displayed in Figure 6. These sensors monitor the systems from a good-as-new state to engine failure. However, sensors 1, 5, 6, 10, 16, 18, and 19 contain little to no information and are thus removed from the analysis. While the dataset provides the potential causes of failure, it does not provide the failure labels. Furthermore, the test set consists of systems for which degradation is only partially observed, together with their corresponding failure times. Therefore, our goal is to use our methodology to predict the remaining life of each testing unit following the final cycle at which their degradation was observed.

Our first step is to perform traditional FPCA on the signals for each sensor. We obtain initial failure mode labels for the training set by applying K-means clustering

TABLE III  
MGR-ASGL performance for case study 1

$SNR_p^k$	FM	Accuracy	Sensors Selected
[2, 5]	1	0.800	1:3, 5, 7:9, 11:16, 18:20
	2	0.875	1, 3:4, 6:10, 13:14, 17:20
[5, 8]	1	0.506	1:7,9:12,14:20
	2	0.669	1:20
[8, 11]	1	0.825	1,3:20
	2	0.788	1:3,5:20

TABLE IV

$l_2$ -norms of four most informative sensors for FM1 & FM2

$SNR_p^k$	FM 1		FM 2	
	Sensor ID	$l_2$ -norm	Sensor ID	$l_2$ -norm
[2, 5]	5	1.809	9	1.667
	12	0.912	7	0.849
	16	0.604	19	0.303
	7	0.269	6	0.218
[5, 8]	5	1.137	9	1.153
	12	0.641	17	0.547
	17	0.500	19	0.537
	18	0.499	4	0.504
[8, 11]	12	1.982	9	2.150
	5	1.422	3	0.559
	16	1.016	19	0.540
	18	0.394	17	0.428

to all FPC-scores. Then, for each sensor, we apply K-means clustering to the FPC-scores associated with that sensor to obtain the covariate information needed to perform CA-FPCA. Following feature extraction, we use 3-fold cross-validation to determine  $(\lambda, \alpha)$ . The range of values for these tuning parameters are identical to that of the simulation case study. The combination of tuning parameters that minimize the mean squared error across the three folds is  $(\lambda_{MSE}, \alpha_{MSE}) = (0.1089, 1)$ . Table VI displays the  $l_2$ -norms of the regression coefficients for each sensor. The sensors selected are those with positive  $l_2$ -norms.

In addition to performing sensor selection, the MGR-ASGL model provides cluster labels for each observed failure. These labels are utilized for the online prediction portion of the methodology. For the online prediction step, we first smooth the degradation signals using 5-fold cross-validation to select the bandwidth parameter. After smoothing, we perform MFPCA on signals from the sensors selected across both failure modes to build our classifier. Then, we classify the failure mode based on the  $0.1N_{t^*}$  nearest neighbors. Given this classification, we perform MFPCA on signals from the sensors selected for the classified failure mode. Finally, we perform Weighted Time-varying Functional Regression to regress  $\ln TTF$  on the MFPC-scores using Leave-one-out cross-validation to select the tuning parameter.

## A. Comparison to Baselines

To analyze our methodology, we compare its performance to that of [37] Chehade et al. (2018), whose methodology assumes knowledge of the failure modes but does not perform sensor selection (outside of removing the blank sensors), and [38] Li et al. (2023), whose methodology assumes knowledge of a fraction of the training set and does perform sensor selection. Figure 7 displays the relative prediction error averaged over all test systems with RUL at most 100, 80, 60, 40, and 20 cycles. From this figure, our methodology becomes

more accurate as the RUL decreases. Furthermore, our methodology is more accurate than both when making longer predictions. For test units whose RUL is at most 20, our accuracy is between that of [37] and [38]. Only at RUL at most 40, does our methodology perform worse than both. To further analyze our methodology, we refer to Figure 8, which displays boxplots showing the distribution of the relative prediction error for test units with remaining life in the following intervals: [0, 25], [26, 50], [51, 75], [76, 100], [101, 125], [126, 150]. The results indicate that our methodology achieves a lower median relative error than [37] in all intervals while maintaining comparable variability. However, the variability for systems with RUL between 25 and 50 is higher for our methodology than for [37]. This indicates a targeted area for improvement of our methodology. However, the general trend is that sensor selection resulted in a more accurate RUL prediction than no sensor selection. Furthermore, we were capable of achieving more accurate RUL prediction than both baselines despite not having information about the actual failure mode.

TABLE V  
Sensors used in case study 2 (C-MAPSS-3 [53])

Sensor ID	Sensor Name	Functionality
1	T2	Total temperature at fan inlet
2	T24	Total temperature at LPC outlet
3	T30	Total temperature at HPC outlet
4	T50	Total temperature at LPT outlet
5	P2	Pressure at fan inlet
6	P15	Total pressure in bypass-duct
7	P30	Total pressure at HPC outlet
8	Nf	Physical fan speed
9	Nc	Physical core speed
10	epr	Engine pressure ratio (P50/P2)
11	Ps30	Static pressure at HPC outlet
12	phi	Ratio of fuel flow to Ps30
13	NRf	Corrected fan speed
14	Nrc	Corrected core speed
15	BPR	Bypass ratio
16	farB	Burner fuel-air ratio
17	htBleed	Bleed enthalpy
18	Nfdmd	Demanded fan speed
19	PCNfRdmd	Demanded corrected fan speed
20	W31	HPT coolant bleed
21	W32	LPT coolant bleed

TABLE VI  
Sensor Selection for Case Study 2

Sensor ID	FM 1	FM2	Sensor ID	FM 1	FM 2
2	0.266	0	12	0	1.148
3	0.584	0	13	0.90	0
4	0.897	0.033	14	0.148	0.119
7	0	0.877	15	0.501	0
8	0.117	0	17	0.230	0.042
9	0.545	0.291	20	0	0.573
11	0	0	21	0.116	0.318

## VIII. CONCLUSION

In this paper, we presented a prognostics methodology tailored to the unique challenges of deep-space habitats. Complex engineering systems such as deep space habitats, are monitored by a large number of sensors and are susceptible to multiple failure modes that are often unlabeled. Our approach addresses the need for autonomous and accurate remaining useful life prediction in environments where expert diagnosis and ground-based maintenance are not feasible.

The methodology consists of two phases. In the offline phase, we extract failure-mode-specific features using component-aligned functional principal component analysis. These features are used by a novel expectation maximization algorithm to train a regression model that simultaneously clusters systems by failure mode and selects the most informative sensors for each mode. In the online phase, we use multivariate functional principal component analysis to reduce the dimensionality of real-time sensor data, diagnose the active failure mode, and predict remaining useful life using a time-varying weighted functional regression model.

We validated our methodology using two case studies. The first is a simulated dataset that reflects key properties of deep-space habitats, including mode-specific degradation behavior, redundant sensors, and variable signal-to-noise ratios. Our method achieved strong performance in clustering failure modes, identifying informative sensors, and predicting remaining useful life with low relative error. The second case study applied our method to the C-MAPSS dataset, which we used to test real-world feasibility under partial degradation observation and unlabeled failure conditions. Our model outperformed baseline approaches in early-life prediction and produced interpretable results by selecting a minimal and relevant set of sensors.

This work is based on the assumption of a linear relationship between the log of time-to-failure (TTF) and the sensor signals. A possibility for improvement would be to relax this assumption. However, embedding a variable selection technique within a nonlinear regression model is an open topic in the literature. Future work will focus on extending the methodology to nonlinear models to improve prediction accuracy and capture complex degradation trends in autonomous mission scenarios.

## REFERENCES

- [1] A. E. Rollock and D. M. Klaus, "Defining and characterizing self-awareness and self-sufficiency for deep space habitats," *Acta Astronautica*, vol. 198, pp. 366–375, 2022.
- [2] S. A. Zaccarine and D. M. Klaus, "Monitoring, maintenance and fault management considerations for self-sufficient deep-space habitat operations," *Acta Astronautica*, vol. 225, pp. 376–389, 2024.
- [3] M. Mirfarah, A. Lund, and S. J. Dyke, "Estimation of pressure leakage severity for space habitats using extended kalman filter," *AIAA Journal*, vol. 63, no. 4, pp. 1615–1628, 2025.

- [4] X. Jin, J. Ni *et al.*, “Physics-based gaussian process for the health monitoring for a rolling bearing,” *Acta astronautica*, vol. 154, pp. 133–139, 2019.
- [5] M. Kordestani, M. E. Orchard, K. Khorasani, and M. Saif, “An overview of the state of the art in aircraft prognostic and health management strategies,” *IEEE Transactions on Instrumentation and Measurement*, vol. 72, pp. 1–15, 2023.
- [6] N. Gebraeel, “Sensory-updated residual life distributions for components with exponential degradation patterns,” *IEEE Transactions on Automation Science and Engineering*, vol. 3, no. 4, pp. 382–393, 2006.
- [7] K. Zhang, Z. Peng, S. Canfei, W. Youren, and C. Zewang, “Remaining useful life prediction of aircraft lithium-ion batteries based on f-distribution particle filter and kernel smoothing algorithm,” *Chinese Journal of Aeronautics*, vol. 33, no. 5, pp. 1517–1531, 2020.
- [8] Z. Wang, W. Wang, C. Hu, X. Si, and J. Li, “A real-time prognostic method for the drift errors in the inertial navigation system by a nonlinear random-coefficient regression model,” *Acta Astronautica*, vol. 103, pp. 45–54, 2014.
- [9] X.-S. Si, W. Wang, C.-H. Hu, D.-H. Zhou, and M. G. Pecht, “Remaining useful life estimation based on a nonlinear diffusion degradation process,” *IEEE Transactions on reliability*, vol. 61, no. 1, pp. 50–67, 2012.
- [10] L. A. Rodríguez-Picón, A. P. Rodríguez-Picón, L. C. Méndez-González, M. I. Rodríguez-Borbón, and A. Alvarado-Iniesta, “Degradation modeling based on gamma process models with random effects,” *Communications in Statistics-Simulation and Computation*, vol. 47, no. 6, pp. 1796–1810, 2018.
- [11] W. Wang, “A prognosis model for wear prediction based on oil-based monitoring,” *Journal of the Operational Research Society*, vol. 58, no. 7, pp. 887–893, 2007.
- [12] H. Pei, X.-S. Si, C. Hu, T. Li, C. He, and Z. Pang, “Bayesian deep-learning-based prognostic model for equipment without label data related to lifetime,” *IEEE Transactions on Systems, Man, and Cybernetics: Systems*, vol. 53, no. 1, pp. 504–517, 2022.
- [13] L. N. Kumari and P. Wang, “Efficient stochastic parametric estimation for lithium-ion battery performance degradation tracking and prognosis,” *Journal of Manufacturing Systems*, vol. 75, pp. 270–277, 2024.
- [14] Y. Zhang, Y. Yang, H. Li, X. Xiu, and W. Liu, “A data-driven modeling method for stochastic nonlinear degradation process with application to rul estimation,” *IEEE Transactions on Systems, Man, and Cybernetics: Systems*, vol. 52, no. 6, pp. 3847–3858, 2021.
- [15] C. Song, K. Liu, and X. Zhang, “A generic framework for multisensor degradation modeling based on supervised classification and failure surface,” *IIEE Transactions*, vol. 51, no. 11, pp. 1288–1302, 2019.
- [16] P. Wen, S. Chen, S. Zhao, Y. Li, Y. Wang, and Z. Dou, “A novel bayesian update method for parameter reconstruction of remaining useful life prognostics,” in *2019 IEEE International Conference on Prognostics and Health Management (ICPHM)*, Jun 2019, p. 1–8.
- [17] L. Gu, Y. Zhou, Z. Zhang, H. Li, and L. Zhang, “Remaining useful life prediction using dynamic principal component analysis and deep gated recurrent unit network,” in *2021 Global Reliability and Prognostics and Health Management (PHM-Nanjing)*, Oct 2021, p. 1–5.
- [18] X. Fang, K. Paynabar, and N. Gebraeel, “Multistream sensor fusion-based prognostics model for systems with single failure modes,” *Reliability Engineering & System Safety*, vol. 159, p. 322–331, Mar 2017.
- [19] M. Kim, C. Song, and K. Liu, “A generic health index approach for multisensor degradation modeling and sensor selection,” *IEEE Transactions on Automation Science and Engineering*, vol. 16, no. 3, p. 1426–1437, Jul 2019.
- [20] F. Lu, J. Wu, J. Huang, and X. Qiu, “Aircraft engine degradation prognostics based on logistic regression and novel os-elm algorithm,” *Aerospace Science and Technology*, vol. 84, pp. 661–671, 2019.
- [21] D. Wang, K. Liu, and X. Zhang, “A generic indirect deep learning approach for multisensor degradation modeling,” *IEEE Transactions on Automation Science and Engineering*, vol. 19, no. 3, p. 1924–1940, Jul 2022.
- [22] C. Che, H. Wang, Q. Fu, and X. Ni, “Combining multiple deep learning algorithms for prognostic and health management of aircraft,” *Aerospace Science and Technology*, vol. 94, p. 105423, 2019.
- [23] N. Li, Y. Lei, N. Gebraeel, Z. Wang, X. Cai, P. Xu, and B. Wang, “Multi-sensor data-driven remaining useful life prediction of semi-observable systems,” *IEEE Transactions on Industrial Electronics*, vol. 68, no. 11, p. 11482–11491, Nov 2021.
- [24] B. Wu, J. Zeng, H. Shi, X. Zhang, G. Shi, and Y. Qin, “Multi-sensor information fusion-based prediction of remaining useful life of nonlinear wiener process,” *Measurement Science and Technology*, vol. 33, no. 10, p. 105106, Jul 2022.
- [25] N. Daroogheh, A. Baniamerian, N. Meskin, and K. Khorasani, “Prognosis and health monitoring of nonlinear systems using a hybrid scheme through integration of pfs and neural networks,” *IEEE Transactions on Systems, Man, and Cybernetics: Systems*, vol. 47, no. 8, p. 1990–2004, Aug. 2017.
- [26] J. Yu, “Aircraft engine health prognostics based on logistic regression with penalization regularization and state-space-based degradation framework,” *Aerospace Science and Technology*, vol. 68, pp. 345–361, 2017.
- [27] Q. Zhang, C. Hua, and G. Xu, “A mixture weibull proportional hazard model for mechanical system failure prediction utilising lifetime and monitoring data,” *Mechanical Systems and Signal Processing*, vol. 43, no. 1, p. 103–112, Feb 2014.
- [28] D. R. Cox, “Regression models and life-tables,” *Journal of the Royal Statistical Society. Series B (Methodological)*, vol. 34, no. 2, p. 187–220, 1972.
- [29] K. Monterrubio-Gómez, N. Constantine-Cooke, and C. A. Vallejos, “A review on competing risks methods for survival analysis,” no. arXiv:2212.05157, Dec 2022, arXiv:2212.05157 [stat].
- [30] X. Zhu, J. Yao, and J. Huang, “Deep convolutional neural network for survival analysis with pathological images,” in *2016 IEEE International Conference on Bioinformatics and Biomedicine (BIBM)*, Dec 2016, p. 544–547.
- [31] G. Gupta, V. Sunder, R. Prasad, and G. Shroff, “Cresa: A deep learning approach to competing risks, recurrent event survival analysis,” in *Advances in Knowledge Discovery and Data Mining*, ser. Lecture Notes in Computer Science, Q. Yang, Z.-H. Zhou, Z. Gong, M.-L. Zhang, and S.-J. Huang, Eds. Cham: Springer International Publishing, 2019, p. 108–122.
- [32] P. Marthin and N. A. Tutkun, “Recurrent neural network for complex survival problems,” *Journal of Statistical Computation and Simulation*, vol. 0, no. 0, p. 1–25, Feb 2023.
- [33] O. O. Aremu, R. A. Cody, D. Hyland-Wood, and P. R. McAree, “A relative entropy based feature selection framework for asset data in predictive maintenance,” *Computers & Industrial Engineering*, vol. 145, p. 106536, Jul 2020.
- [34] M. Kim and K. Liu, “A bayesian deep learning framework for interval estimation of remaining useful life in complex systems by incorporating general degradation characteristics,” *IIEE Transactions*, vol. 53, no. 3, p. 326–340, Mar 2021.
- [35] R. Jiao, K. Peng, J. Dong, and C. Zhang, “Fault monitoring and remaining useful life prediction framework for multiple fault modes in prognostics,” *Reliability Engineering & System Safety*, vol. 203, p. 107028, Nov. 2020.
- [36] J. Xiong, J. Zhou, Y. Ma, F. Zhang, and C. Lin, “Adaptive deep learning-based remaining useful life prediction framework for systems with multiple failure patterns,” *Reliability Engineering & System Safety*, vol. 235, p. 109244, Jul. 2023.
- [37] A. Chehade, C. Song, K. Liu, A. Saxena, and X. Zhang, “A data-level fusion approach for degradation modeling and prognostic analysis under multiple failure modes,” *Journal of Quality Technology*, vol. 50, no. 2, p. 150–165, Apr 2018.

- [38] H. Wu and Y.-F. Li, "A multi-sensor fusion-based prognostic model for systems with partially observable failure modes," *IJSE Transactions*, vol. 0, no. ja, p. 1–21, Jun 2023.
- [39] Y. Fu, Y. Kwon Huh, and K. Liu, "Degradation modeling and prognostic analysis under unknown failure modes," *IEEE Transactions on Automation Science and Engineering*, vol. 22, pp. 11 012–11 025, 2025.
- [40] Y. Su and X. Fang, "Deep learning-based residual useful lifetime prediction for assets with uncertain failure modes," *Journal of Computing and Information Science in Engineering*, pp. 1–29, 2025.
- [41] C. Song, K. Liu, and X. Zhang, "A generic framework for multisensor degradation modeling based on supervised classification and failure surface," *IJSE Transactions*, vol. 51, no. 11, p. 1288–1302, Nov 2019.
- [42] H. Li, W. Zhao, Y. Zhang, and E. Zio, "Remaining useful life prediction using multi-scale deep convolutional neural network," *Applied Soft Computing*, vol. 89, p. 106113, Apr 2020.
- [43] E. Giunchiglia, A. Nemchenko, and M. van der Schaar, "Rnn-surv: A deep recurrent model for survival analysis," in *Artificial Neural Networks and Machine Learning – ICANN 2018*, ser. Lecture Notes in Computer Science, V. Kůrková, Y. Manolopoulos, B. Hammer, L. Iliadis, and I. Maglogiannis, Eds. Cham: Springer International Publishing, 2018, p. 23–32.
- [44] P. Wang, Y. Li, and C. K. Reddy, "Machine learning for survival analysis: A survey," *ACM Computing Surveys*, vol. 51, no. 6, pp. 110:1–110:36, Feb 2019.
- [45] Y. Wang, L. Deng, L. Zheng, and R. X. Gao, "Temporal convolutional network with soft thresholding and attention mechanism for machinery prognostics," *Journal of Manufacturing Systems*, vol. 60, pp. 512–526, 2021. [Online]. Available: <https://www.sciencedirect.com/science/article/pii/S027861252100145X>
- [46] C.-R. Jiang and J.-L. Wang, "Covariate adjusted functional principal components analysis for longitudinal data," *The Annals of Statistics*, vol. 38, no. 2, p. 1194–1226, 2010.
- [47] K. Karhunen, *Über lineare Methoden in der Wahrscheinlichkeitsrechnung*. Kirjapaino oy. sana, 1947, google-Books-ID: bGU-UAQAIAAJ.
- [48] F. Yao, H.-G. Müller, and J.-L. Wang, "Functional data analysis for sparse longitudinal data," *Journal of the American Statistical Association*, vol. 100, no. 470, p. 577–590, Jun 2005.
- [49] N. Städler, P. Bühlmann, and S. van de Geer, "L1-penalization for mixture regression models," *TEST*, vol. 19, no. 2, p. 209–256, Aug 2010, arXiv:1202.6046 [stat].
- [50] W. S. Cleveland, "Robust locally weighted regression and smoothing scatterplots," *Journal of the American Statistical Association*, Apr 2012. [Online]. Available: <https://www.tandfonline.com/doi/abs/10.1080/01621459.1979.10481038>
- [51] H.-G. Müller and Y. Zhang, "Time-varying functional regression for predicting remaining lifetime distributions from longitudinal trajectories," *Biometrics*, vol. 61, no. 4, pp. 1064–1075, 2005.
- [52] X. Fang, R. Zhou, and N. Gebraeel, "An adaptive functional regression-based prognostic model for applications with missing data," *Reliability Engineering & System Safety*, vol. 133, p. 266–274, Jan 2015.
- [53] A. Saxena, K. Goebel, D. Simon, and N. Eklund, "Damage propagation modeling for aircraft engine run-to-failure simulation," in *2008 International Conference on Prognostics and Health Management*, Oct. 2008, p. 1–9.
- [54] K. P. Murphy, *Machine learning: a probabilistic perspective*. MIT press, 2012.

## Appendix

DEFINITION 1 The log-likelihood function for the MGR model is given by equation (25). This function is called as the "incomplete-data log-likelihood" (IDLL), since we

do not know the cause of the observed failure in the data.

$$\ell(\Theta; \mathbf{Y}) = \sum_{i=1}^N \ln \sum_{k=1}^K \pi_k \frac{\rho_k}{\sqrt{2\pi}} \exp\left(-\frac{1}{2}(\rho_k y_i - \psi_{0,k} - \sum_{p=1}^P \mathbf{x}_{i,p}^T \boldsymbol{\psi}_{p,k})^2\right) \quad (25)$$

DEFINITION 2 The "complete-data log-likelihood" (CDLL) given by equation (26) assumes knowledge of the underlying causes of the observed failure in the data.

$$\ell_C(\Theta; \mathbf{Y}, \mathbb{Z}) = \sum_{i=1}^N \sum_{k=1}^K \mathbf{Z}_i[k] \ln \pi_k \left(\frac{\rho_k}{\sqrt{2\pi}}\right) \times \exp\left(-\frac{1}{2} \left(\rho_k y_i - \psi_{0,k} - \sum_{p=1}^P \mathbf{x}_{i,p}^T \boldsymbol{\psi}_{p,k}\right)^2\right) \quad (26)$$

The IDLL given in equation (25) is difficult to optimize globally [54]. Instead, we search for a local optimum by using EM algorithm, an iterative algorithm suitable for fitting probability models with latent variables. To derive the steps of the EM algorithm, we note that since  $\ln(\cdot)$  is a concave function We use Jensen's inequality to form a lower bound on the IDLL. This lower bound is the expectation of the CDLL given in equation (26) and shown in Lemma 1.

LEMMA 1 *The expectation of the CDLL w.r.t distribution  $g$  is a lower bound for the IDLL i.e.,*

$$\mathbb{E}_g[\ell_C(\Theta; \mathbf{Y}, \mathbb{Z})] \leq \ell(\Theta; \mathbf{Y})$$

*Proof:*

Let  $g$  be an arbitrary distribution on  $\mathbf{Z}_i[k]$ . Then we can re-write equation (25) as follows:

$$\begin{aligned} \ell(\Theta; \mathbf{Y}) &= \sum_{i=1}^N \ln \left( \sum_{k=1}^K \frac{g(\mathbf{Z}_i[k]) p(y_i, \mathbf{Z}_i[k]; \Theta)}{g(\mathbf{Z}_i[k])} \right) \\ \text{where,} & \\ p(y_i, \mathbf{Z}_i[k]; \Theta) &= \pi_k \cdot \left( \frac{\rho_k}{\sqrt{2\pi}} \exp\left(-\frac{1}{2} \left(\rho_k y_i - \psi_{0,k} - \sum_{p=1}^P \mathbf{x}_{i,p}^T \boldsymbol{\psi}_{p,k}\right)^2\right) \right) \end{aligned}$$

Since  $\ln(\cdot)$  is concave, from Jensen's inequality we can write that,

$$\ell(\Theta; \mathbf{Y}) \geq \sum_{i=1}^N \sum_{k=1}^K g(\mathbf{Z}_i[k]) \ln \frac{p(y_i, \mathbf{Z}_i[k]; \Theta)}{g(\mathbf{Z}_i[k])}$$

and thus,

$$\ell(\Theta; \mathbf{Y}) \geq \mathbb{E}_g[\ell_C(\Theta; \mathbf{Y}, \mathbb{Z})] - \sum_{i=1}^N \sum_{k=1}^K g(\mathbf{Z}_i[k]) \ln g(\mathbf{Z}_i[k])$$

The second term on the right side of the inequality is the negative entropy of the  $g$  distribution. Since it is positive, the inequality holds. ■